

A248: Magneto-optical Trap

Bence Mitlasóczy*and Benoît Scholtes†
Rheinische-Friedrich-Wilhelms Universität Bonn

March 26, 2018

We adjusted some mirrors to get MOT. We did some measurements.

1 Introduction

Magneto-optical traps (MOT) are an important apparatus in modern atomic physics experiments, used to slow and trap a neutral atom cloud to temperatures as cold as several microkelvin. They are achieved by combining radiation pressure from laser beams and a quadrupole magnetic field inside a vacuum cell rid of other gasses. Their use ranges from probing atomic properties, quantum optics, cold collision, quantum information processing, and acting as the preliminary stage to achieving even colder atom traps, namely Bose-Einstein condensates. This experiment aimed at obtaining a MOT and finding its size, population, and loading behaviour as well its fluorescence dependence on the magnetic field strength, quarter waveplate angle, and laser frequency detuning.

2 Theory

The central process by which atomic gasses are cooled are via radiation pressure from lasers. When a photon is absorbed by an object, particle, or atom, its energy as well as its momentum, equal to $p = \hbar k$, is absorbed as a result of momentum conservation. This radiation pressure can be used to slow down moving atoms if the atoms absorb photons travelling in the opposite direction. The atoms are thus cooled due to the decrease in their kinetic energy, which is proportional to their temperature. Only photons resonant to a transition of the absorption spectrum of the atoms are absorbed however. As a result, the absorption spectrum of the atoms to be cooled needs to be known and a particular transition chosen such that the required frequency of the cooling laser can be determined. The absorption spectrum of ^{85}Rb and the transition used is discussed in Section 2.5.

A moving atom will no longer be able to absorb photons with frequencies from the absorption spectrum however, as their frequency will be Doppler shifted and no

longer resonant to the atom transitions. The moving atom will only be able to absorb light which has been Doppler shifted such that it is resonant with one of its excitation transitions. In an uncooled gas, the atoms are all travelling in different directions with different speeds. As a result, light incident on the gas from a single direction will be Doppler shifted differently for all the different atoms. An absorption spectrum obtained from such a gas will thus be Doppler broadened, making it difficult to determine the energy levels and transitions of the atoms. In order to obtain a spectrum with high resolution, Doppler-free spectroscopy such as saturation spectroscopy needs to be used.

2.1 Saturation Spectroscopy

Atoms can only absorb photons with frequencies that are resonant to their excitation transitions. That said, a moving atom will not be able to absorb photons with these frequencies as their frequency will be Doppler shifted and no longer resonant to the atom transitions. The moving atom will only be able to absorb light which has been Doppler shifted such that it is resonant with one of its excitation transitions. In an uncooled gas, the atoms are all travelling in different directions with different speeds. As a result, light incident on the gas from one direction will be Doppler shifted differently for all the different atoms. An absorption spectrum obtained from such a gas will thus be Doppler broadened, making it difficult to determine the energy levels and transitions of the atoms. In order to obtain a spectrum with high resolution, Doppler-free spectroscopy such as saturation spectroscopy needs to be used.

Saturation spectroscopy utilises two lasers, called the pump and test beams, which are incident on the gas in opposite directions. The test beam is much less powerful and its intensity after passing through the gas is measured.² The absorption spectrum measured in this manner will largely look like a Doppler broadened spectrum, though with sharp peaks in the middle of Doppler broadened peaks as seen in Figure 1. These are a result of the intense pump beam directed in the opposite di-

*s6bemitl@uni-bonn.de

†s6bescho@uni-bonn.de

rection though always with the same frequency as the test beam. Only atoms stationary along the axis of the lasers will be resonant to both the pump and test beam for a given transition as the Doppler shifts of either laser is always different for moving atoms. As a result, when the pump and test beam are resonant to an excitation transition, the pump beam will saturate the stationary atoms by exciting most of them to higher states, leaving few left for the test beam to excite. Thus the test beam will be measured with a much less diminished intensity than was measured for other frequencies, where the atoms saturated by the pump beam were not those resonant to the test beam. Thus a peak in the Doppler broadened absorption spectrum is observed, called a Lamb dip. These peaks provide the frequencies of the Doppler-free absorption spectrum of the gas. A crossover peak is observed when the pump and test beam are both resonant to atoms moving at such a velocity that two different hyperfine transitions are individually resonant to both beams. Here, the pump beam excites many atoms to a certain state, thereby depopulating the ground state of these atom and again leaving few left for the test beam to excite. This leads to more peaks in the absorption spectrum than the number of transitions.

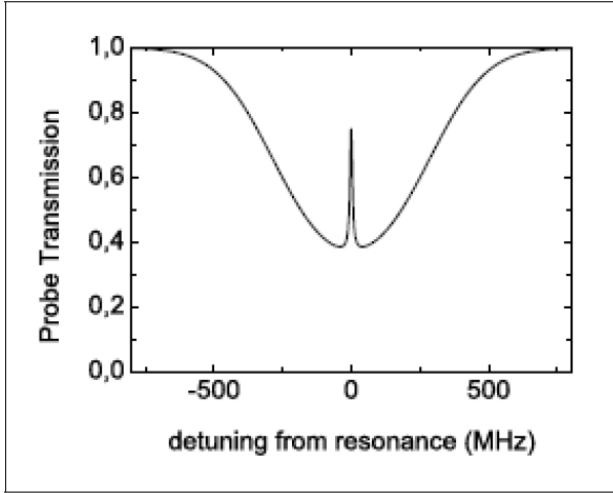


Figure 1: A Lamb dip observed in a Doppler-broadened absorption peak.²

2.2 Polarisation Spectroscopy

Polarization spectroscopy expands on saturation spectroscopy. The pump beam is circularly polarized with a quarter waveplate before entering the sample. This introduces anisotropy in the populations of the degenerate magnetic hyperfine states of the atoms and as a result the sample becomes birefringent.⁷ In the realised set-up, the linearly polarised probe beam is split in two beams by a polarizing beam splitter (PBS). One of the beams then passes through the birefringent sample

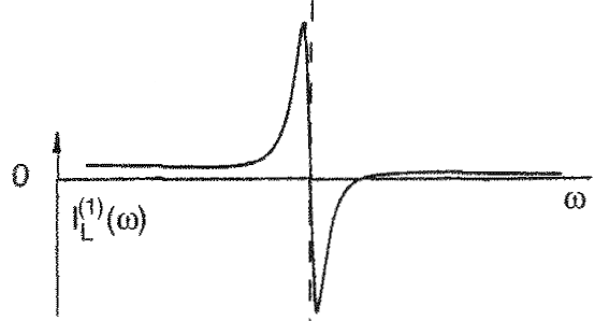


Figure 2: An example of a dispersive signal used as the error signal for locking the cooling laser.⁷

which tilts its polarization axis slightly. Both beam signals are then detected and their difference is taken to determine the axis shift. The result is a dispersive signal with a shape similar to what is shown in Figure 2. The zero crossing with differing voltage signs on the two sides provides a precise locking point for the cooling and repumping laser frequencies and is thus used as the error signal, discussed in Section 2.6. This stabilises the frequencies of the lasers such that a MOT can be more easily obtained and held.

2.3 Optical Trap

An optical trap is organised with three lasers for the three directions of space, orientated so that they have a crossing point. Each laser is then reflected back into the gas and through this central crossing point so that there are six counter-propagating beams. This provides radiation pressure in six different directions, all directed back toward the crossing point. That said, the radiation pressure should only be imposed on atoms moving away from the trap. Otherwise, the lasers would also push out atoms in the trap and along the laser beam. As a result, the lasers are all red detuned from a particular transition such that when the atoms are moving away from the trap, these lasers are blueshifted for the atoms and become resonant with the transition allowing for the absorption of the photons. That said, the resonance of the atoms with the lasers is dependent on the velocity of the atoms. Furthermore, the probability of an atom absorbing a photon is dependent on the difference between the Doppler shifted frequency of the photon and the atom's transition frequency, as show in Figure 3. It can be seen that more atoms moving away from the centre will be forced back than atoms moving toward the centre. That said, using only one frequency for the lasers means that many atoms moving away from the centre of the trap will still be largely transparent to the lasers due to small scattering rates. The optical trap purely achieves an “optical molasses” in the intersection volume of the lasers, so called because atoms moving away from the centre are slowed as if moving in a viscous medium. This

molasses cannot completely stop the atoms from leaving the intersection volume however, whereby they will be lost to the trapping method, nor does it provide a point that the atoms are drawn towards. As a result, using the optical trap in conjunction with a magnetic trap is a better method.

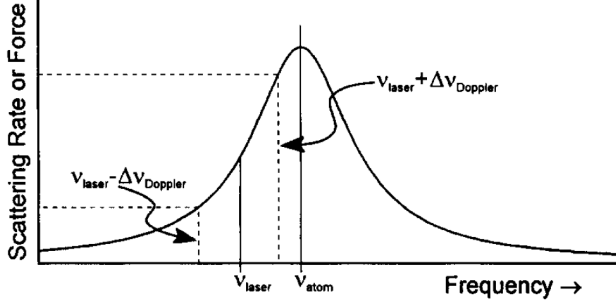


Figure 3: The scattering rate and thus force from radiation pressure between the differently Doppler shifted laser photons and the atoms.⁴

2.4 Magneto-optical Trap

A magnetic field is used to introduce a position-dependent force from radiation pressure. Two coils are arranged in an anti-Helmholtz configuration (face to face but with currents in opposing directions) to produce a quadrupole magnetic field, pictured in Figure 4. This

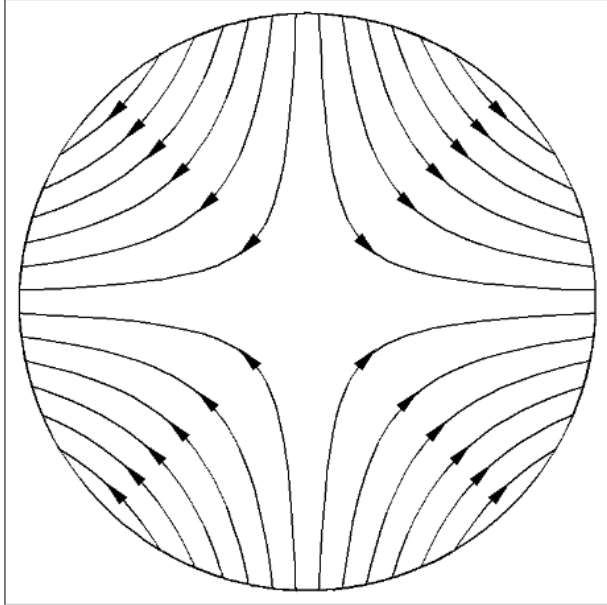


Figure 4: A quadrupole magnetic field in 2D space. The field lines become more dense further from the centre, showing the increase in magnetic field strength.⁵

magnetic field has a strength that increases linearly from centre, which itself has zero magnetic field. This means

that the Zeeman effect, which splits previously degenerate magnetic energy levels of atoms into non-degenerate states with separation proportional to magnetic field strength $\Delta E \propto m_i B$ (where m is the magnetic quantum number), increasingly separates energy levels the further from the centre an atom is. The lasers can thus be red detuned from one of these transitions such that as an atom moves away from centre, the transition becomes increasingly resonant with the laser, increasing the scattering rate. As a result, the force felt by atoms moving away from the centre of the intersection volume increases with distance, such that atoms can be more effectively trapped. This also ensures that atoms in centre of the volume will be largely transparent to the cooling lasers, as there is no magnetic field. Figure 5 illustrates the Zeeman effect and resulting force on the atoms on either side of the trap. As the magnetic field has a different

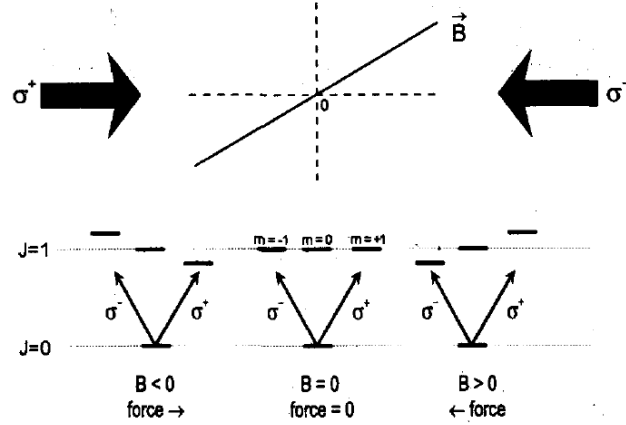


Figure 5: The Zeeman effect on atoms on either side of the centre where the magnetic field changes sign. The transitions allowed for differently polarised light is also shown.⁴

sign on either side of the centre, a certain energy level m_i will not have the same energy on either side. Circularly polarised lasers therefore need to be used, where the reflection of a laser will cause the polarisation to flip from σ_- to σ_+ for example. The counter-propagating laser beams are thus oppositely polarised meaning that they will be resonant with different transitions, one with $m = -1$ and the other with $m = +1$. This is due to the transition selection rules where a σ_{\pm} polarised photon requires that $\Delta m = \pm 1$ between the initial and final states of the atom.⁶ Though the beams are resonant to different transitions, these transitions will have the same energies the same distance away from the centre, meaning that a laser with a single frequency can become increasingly resonant atoms on either side of the atom trap. The magnetic field has thus introduced a point which the atoms are drawn towards. The complete MOT set-up is given in Figure 6. The centre of the magnetic field is to be aligned with the centre of the intersection volume of the lasers to achieve the best results.

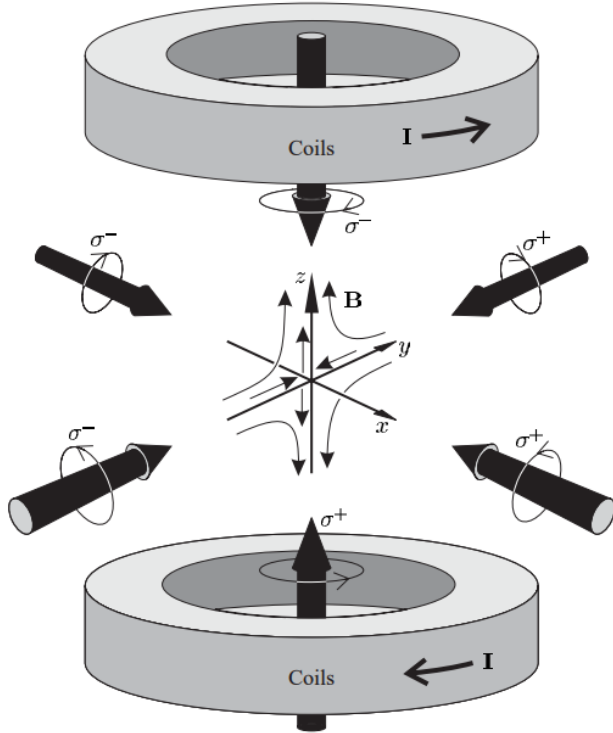


Figure 6: The MOT set-up, shown with the coils in anti-Helmholtz configuration, magnetic field, and laser beam polarisations.⁶

There is a limit to the extent that a MOT can cool down atoms. The atoms must always re-emit the energy that they have absorbed from the lasers. These photon emissions are isotropic however, leading to an average recoil force on the atom of $\langle F \rangle_{\text{recoil}} = 0$ N, retaining the efficiency of the optical trap method. The atoms will nevertheless be pushed around randomly by the recoil forces during each photon emission, thus meaning that the kinetic energy and consequently temperature of the atoms will not be able to be further reduced past this point. This minimum temperature is called the Doppler limit, which is generally in the μK for an MOT. Methods such as Bose-Einstein condensation must be used to cool down atom traps further.

2.5 Rubidium

Natural Rubidium gas is composed of ^{85}Rb and ^{87}Rb . This experiment focuses on ^{85}Rb as it is approximately three times more abundant in the gas. The level structure of ^{85}Rb is given in Figure 7. The transition used in this experiment for resonance with the cooling lasers with σ_+ polarisation is the $F=3$ (or $m=3$) $\rightarrow F'=4$ transition. This transition is nominally closed meaning that excited atoms can only decay down into the $F=3$ state. This means that are continuously able to absorb photons from the cooling lasers, allowing for further cooling and

trapping. There are rare excitations to the $F'=2,3$ states however which can decay to the $F=2$ ground state which is no longer resonant to the cooling lasers. As a result, a repumping laser tuned to the $F=2 \rightarrow F'=3$ transition is introduced to pump atoms back into states sensitive to the cooling lasers when they decay to the $F=3$ state. One should note that ^{87}Rb is still present in the gas and that its spectrum will be visible.

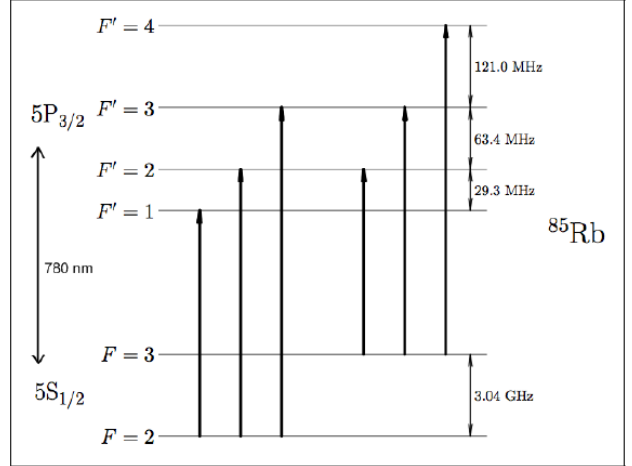


Figure 7: The energy levels $5S_{1/2}$ and $5P_{1/2}$ of ^{85}Rb . The cooling laser and repumping laser transitions used are the $F=3 \rightarrow F'=4$ and $F=2 \rightarrow F'=3$ transitions respectively.⁴

2.6 Diode Laser

Diode lasers are used in this experiment for the cooling and repumping lasers. The reasons for this are that the state transitions we exploit for cooling and repumping lie in the infrared range and that we need tunable coherent light sources. Diode lasers work via the recombination of an electron with a hole in a diode, resulting in electromagnetic radiation with a large linewidth, which starts the laser oscillations.⁷ In the laser diode, the metal case used for heat dissipation and the optical cavity makes it possible that population inversion can occur above a threshold current, which means a large free spectral range can be lased. In order to produce a laser with a single mode instead, a grating is used as shown in Figure 8. Here, the laser produced by the diode is divergent and collimated to a non-divergent beam by the collimating lens. The beam is then directed on to an external grating in Littrow configuration, as seen in Figure 9. The grating is positioned such that for the desired frequency, the -1 . order is reflected back into the active medium, thus serving as an external resonating element. This back-reflected frequency determines the single-mode frequency of the laser. The actual beam produced for use is the 0 . order, which makes up most of the produced power of the laser diode. For constructive interference, the grating equation reads as given in Figure 9, such that a

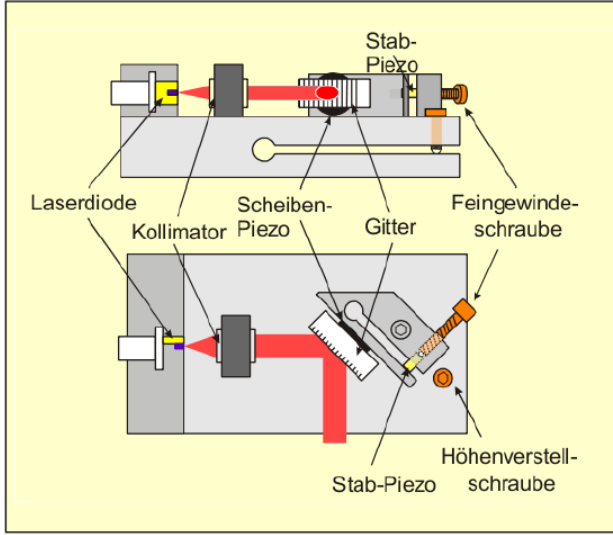


Figure 8: The diode laser with the grating in Littrow configuration.²

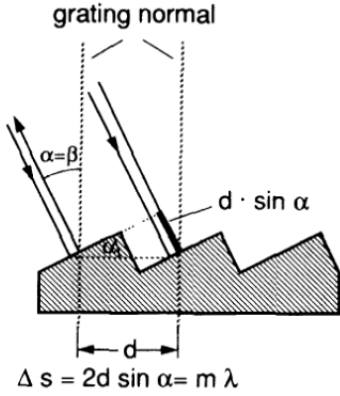


Figure 9: Diffraction grating in a Littrow configuration, when the incident and reflected beams coincide.⁷

single mode is obtained. A piezo system functioning on triangular supply voltage, as well as adjustable screws, are responsible for the moving of the grating so that different frequencies in the laser spectrum can be reflected back to the laser, allowing for frequencies of the laser to be scanned. The error signal produced by polarisation spectroscopy, discussed in Section 2.2, is that used as the triangular voltage to stabilise and lock the laser to a desired frequency. The frequency can also be changed with the current applied to the diode and the diode's temperature, such that changes in the temperature of the room causes the frequency of the laser to drift.

3 Experimental Set-up

The laser section of the experiment is shown in Figure 10. This produces both cooling and repumping lasers which are sent to the MOT set-up collinear through

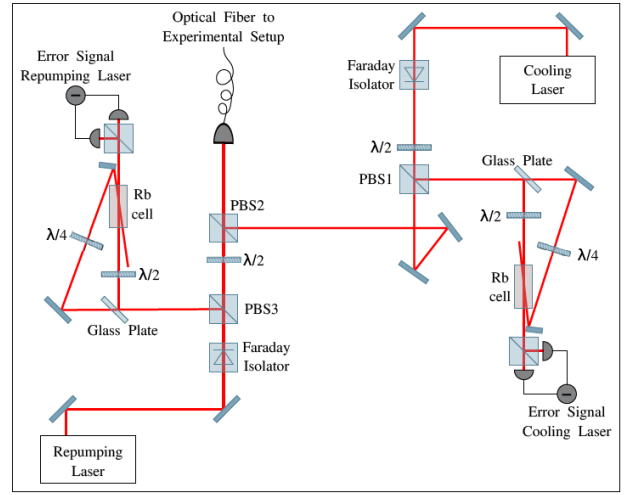


Figure 10: The set-up for producing the cooling and repumping lasers, sent to the MOT experiment.²

an optical fibre. Two cells with Rubidium gas are used for the polarisation spectroscopy to produce the error signals to scan and lock both lasers. This part of the experiment was already configured.

3.1 MOT Set-up and Procedure

The MOT set-up is shown in Figure 11. A va-

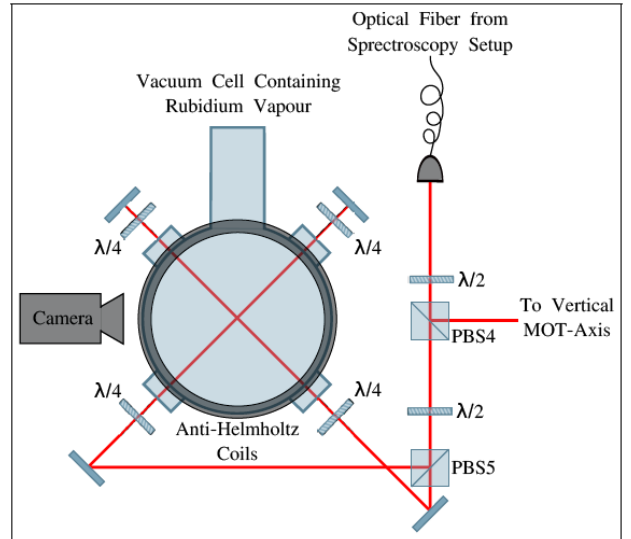


Figure 11: The MOT set-up.²

cuum chamber held at pressure levels of approximately 10^{-7} mbar with glass windows served as the container for the Rubidium gas. The collinear cooling and repumping beams were directed by two beam splitters, several mirrors, and six quarter waveplates for each of the beams convergent on the atom trap. The six beams could be adjusted by fine-tuning the mirror angles with screws.

The two coils which provided the magnetic field were fixed in space, thus providing a fixed magnetic field. The strength of the magnetic field could be altered however, by changing the current applied to the coils. Acquiring a MOT was the first aim of the experiment. To do so, the six laser beams had to be aligned such that they formed an intersection volume in the centre of the magnetic field. Markings on the vacuum cell container gave approximate indications of the centre of the magnetic field. An infrared camera was also used to see the fluorescence of the laser beams in the vacuum cell and thus the laser beams themselves. Using these two devices, the beams were aligned to cross approximately at the centre of the magnetic field. It was necessary to make sure that none of the laser beam profiles were cut so that as little power was lost. Furthermore, in order to make sure that the laser beams were reflected adequately back into the gas along the beams of the incident lasers, the mirrors were fine-tuned so that the beams were reflected back into the optical fibre. This was achieved by using a piece of paper with a small hole in it to allow the incident beam near the optical fibre to pass through and seeing on the paper how far the reflected beams were from being reflected perfectly back through the hole. The mirrors were adjusted until this was achieved.

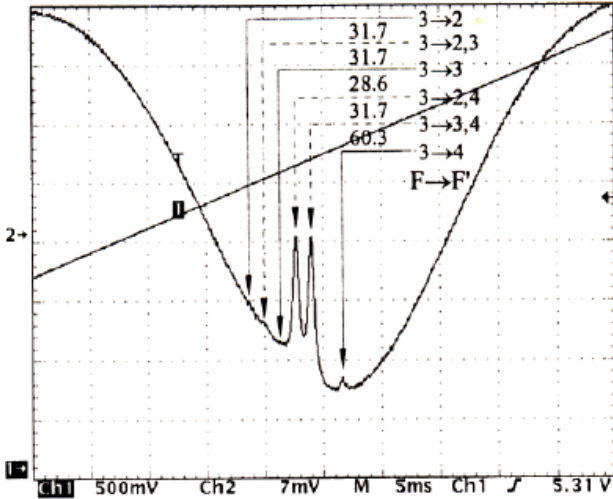


Figure 12: ^{85}Rb observed spectrum with Lamb dips for $F = 3 \rightarrow F' = 2, 3, 4$. The transitions to states with two numbers refer to crossover peaks.²

Once an intersection was accomplished, the spectrum of the gas was obtained on an oscilloscope by scanning the cooling laser, as shown in Figure 12. When the peak for the desired $F=3 \rightarrow F'=4$ transition was found, the laser was locked to a frequency slightly red detuned from this as a guess. For the repumping laser, the $F=2 \rightarrow F'=3$ transition was found in the spectrum, shown in Figure 12, and the laser was made to scan a small range over the peak. The laser was not detuned as it is not

used to cool the atoms, just to repump atoms lost to the cooling process. Furthermore, it was not locked for most of the experiment as it was found that a large MOT was obtained when it was made to scan a small range. This is thought to be due to the ability for the laser to be resonant with more atoms of different speeds and different positions in the magnetic field. The frequencies of the la-

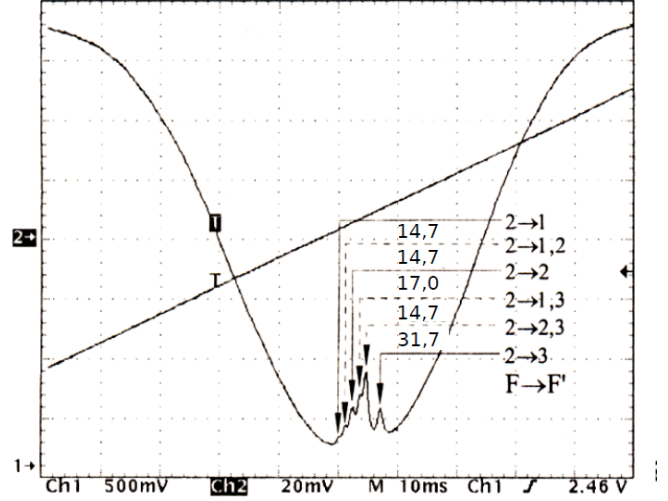


Figure 13: ^{85}Rb observed spectrum with Lamb dips for $F = 2 \rightarrow F' = 1, 2, 3$. The transitions to states with two numbers refer to crossover peaks.²

sers were then finely tuned, especially that of the cooling laser, until a MOT was observed by a video camera able to see the infrared fluorescence emitted. A ferromagnet was also used to affect the magnetic field of the coils to see whether a MOT could be observed. This would suggest that the intersection point of the laser beams were not properly aligned with the centre of the magnetic field and that they needed to be re-aligned. Once a lasting MOT was observed with adequate luminescence, the quantitative measurements were undertaken. Due to the laser drift caused by the ambient temperature change, the measurements had to be performed quickly.

4 Results

4.1 Laser Beam Diameter

Using a movable razor blade and a powermeter, the intensity of the combined cooling and repumping laser beam as a function of the displacement of the blade along an axis perpendicular to the beam propagation, thereby blocking parts of the beam, was measured. The results are collected in Table 1. The uncertainty in the power measurements is a result of their sensitivity to very slight movements of the blade, less than was noticeable. The errors were estimated to be approximately 5% for all values by repeating measurements of different values and

Position (cm)	Power (mW)
39.4 ± 0.05	1.58 ± 0.08
39.5 ± 0.05	1.57 ± 0.08
39.6 ± 0.05	1.52 ± 0.08
39.7 ± 0.05	1.40 ± 0.07
39.8 ± 0.05	1.07 ± 0.05
39.9 ± 0.05	0.62 ± 0.03
40.0 ± 0.05	0.25 ± 0.01
40.1 ± 0.05	0.10 ± 0.01
40.2 ± 0.05	0.04 ± 0.01
40.3 ± 0.05	0.01 ± 0.01
40.4 ± 0.05	$0.00^{+0.01}_{-0.00}$

Table 1: Beam power as a function of position of the razor blade. The last value has no negative uncertainty as the powermeter didn't read a negative value in this mode, even when it was blocked from light. The last few readings have higher uncertainty due to larger reading fluctuations observed.

quantifying their deviation. Fitting a function of the form

$$f(x) = P + A \cdot \text{erfc}(B \cdot x - C),$$

we found

$$\begin{aligned} P &= 0.0066 \pm 0.0005, \\ A &= 0.748 \pm 0.016, \\ B &= 4.681 \pm 0.095, \\ C &= 187.6 \pm 3.8. \end{aligned}$$

This results in a width of the laser beam of

$$w = 0.2860 \text{ cm} \pm 0.0077 \text{ cm}.$$

The results with the fit are plotted in Figure 14.

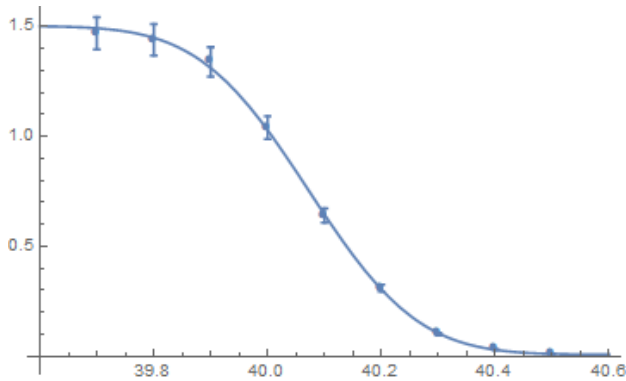


Figure 14: Plot of the laser beam luminosity with razor blade position, provided with fit.

4.2 Size of the MOT

To get an estimate of the MOT size, we took a photo of it from the side, shown in Figure 15. The photo is superimposed with a photo of a ruler placed the same distance

away from the camera as the MOT. This was achieved by moving the ruler back and forth until it was in the focus of the camera and was done so that a scale for the MOT image could be used to convert distances in pixels to centimetres. The MOT as well as the vertical and horizontal

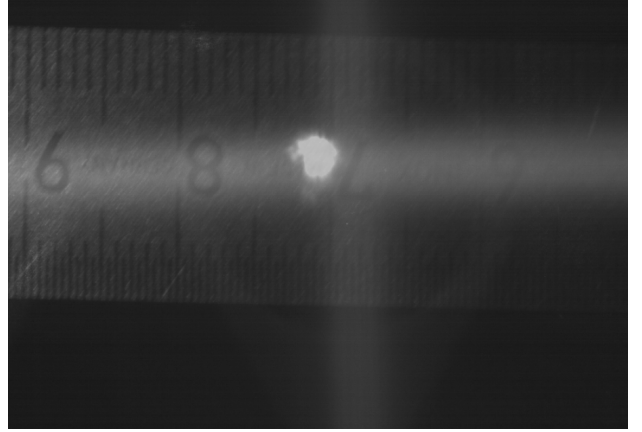


Figure 15: Photo of the MOT merged with photo of the scale.

laser beams can be seen in the photo. An image software determined that two points (30.0 ± 0.5) mm away from each other in the image were separated by 742.2 pixels. The uncertainty here is due to the width of the millimetre lines on the scale and the two points not at the same distance from the edge of the ruler. Thus

$$1 \text{ px} = (40.42 \pm 0.67) \mu\text{m}.$$

As visible in Figure 15, the MOT does not have a perfect circular cross-section. This is likely the result of the laser beams not intersecting to form a perfect cubic intersection volume and not being exactly centred with the magnetic field. The latter can be directly observed in the photo from the discrepancy between the position of MOT and the centre of the intersection of the beams. The directly measured width and height for the MOT are

$$h = (72 \pm 2) \text{ px}, \text{ and } w = (57 \pm 2) \text{ px}.$$

We chose to approximate the volume by an ellipsoid with one axis half the height (c) and two axes half the width (a, b) each, as our best guess is that the MOT is just as deep as it is wide. That said, the imaged cross-section of the MOT is nearly circular thereby giving more some assurance that the real depth wasn't too different from our estimation. The dimensions of the MOT and its volume were calculated to be

$$\begin{aligned} a, b &= (1.15 \pm 0.04) \text{ mm}, \\ c &= (1.46 \pm 0.05) \text{ mm}, \\ V &= \frac{4}{3} \pi abc = (8.09 \pm 0.52) \text{ mm}^3. \end{aligned}$$

4.3 Magnetic Field Dependence

To measure the MOT fluorescence as a function of the magnetic field, we changed the current flowing through the coils. The luminosity of the fluorescence was measured with a powermeter directed at the MOT. Figure 16 shows our results. The plot seems to suggest that the

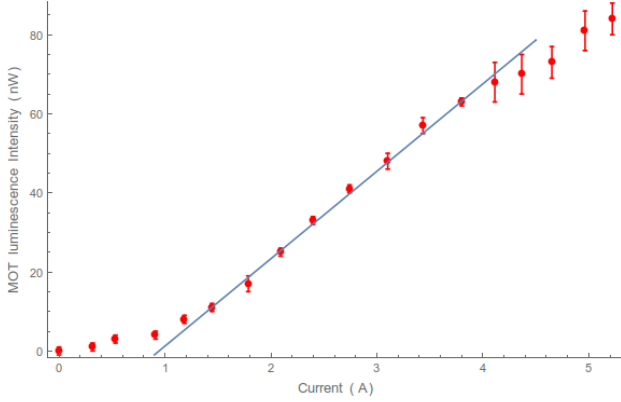


Figure 16: The dependency of MOT luminosity on the current flow through the coils and thus the strength of the magnetic field, given with linear fit.

MOT luminosity follows a sigmoid curve relationship with magnetic field strength, though it is nearly linear. To get a visible MOT, we had to set the current to a minimal value of around 0.9 A. From this point, it can be seen that the fluorescence grew approximately proportional to the current, up to 4.6 A. The background fluorescence from the lasers and the environment was previously measured and subtracted from the data. A linear fit was performed for the central linear section, with calculated coefficients $a = 22.11 \pm 0.53$ nW/A and $\text{const} = -20.9 \pm 1.5$ nW. It can be seen that the full plot is not linear. Further experiments can aim at obtaining a more luminous MOT in order to determine whether this relationship is indeed linear or sigmoid-like, or neither.

4.4 Influence of Quarter Waveplate

The influence of the quarter waveplate angles were then measured. Firstly, the angle of the quarter waveplate for one of the beams before it first passes through the vacuum cell was scanned. This is illustrated as one of the two quarter waveplates on the lower half of Figure 11. Changing this quarter plate thus also affects the polarisation of the reflected beam, given that the relative angle between the two waveplate changes. The powermeter was again used to measure the MOT luminosity. The background luminosity was not subtracted from the data as it was found that it fluctuated in time, meaning that it was not a systematic shift in the data. The reason for the fluctuations are unknown. A plot of the results with a periodic fit is given in Figure 17. The

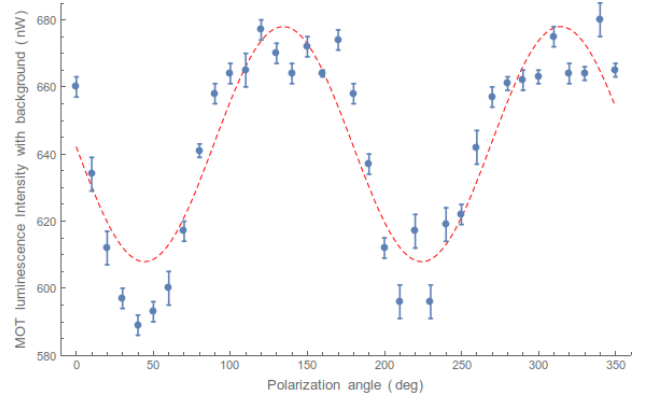


Figure 17: MOT luminescence intensity as a function of the polarization angle of the first quarter waveplate.

function of the fit is

$$f(x) = A \cos(x - \varphi) + B,$$

which produced coefficients

$$A = 70.0 \pm 5.5,$$

$$B = 607.9 \pm 3.8,$$

$$\varphi = ??? \pm 0.095.$$

The angle of the second quarter waveplate after the beam was reflected back into the vacuum cell was then scanned. Changing this waveplate does not affect the polarisation of the incident beam obviously, thus serving as a different investigation to the one above. The results are displayed in Figure 18. Here, the strong fluctuations in the values make it impossible to notice fine angle-dependent changes. The underlying function

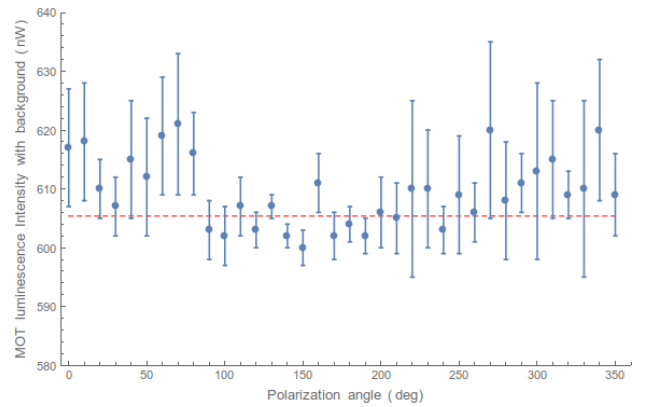


Figure 18: MOT luminescence intensity as a function of the polarization angle of the second quarter waveplate, given with a fit.

most likely appears to be a constant function, shown as the

red dashed fitted line. Further experiments could determine whether this relationship is indeed linear by achieving a more stable MOT, allowing for a more accurate determination of the relationship.

4.5 Loading Behaviour

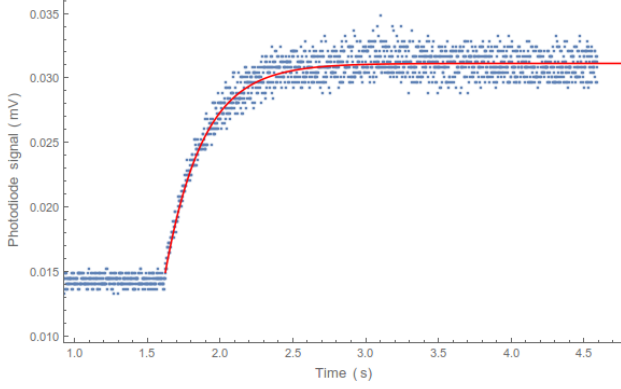


Figure 19: Example of data points exported from the oscilloscope, with fitted function (red).

After replacing the powermeter with a photodiode and showing its signal on an oscilloscope, we used the data from 6 MOT buildup events to find the loading time. As it is known,¹ the number of trapped atoms changes as

$$N(t) = N_0(1 - e^{-\frac{t}{\tau}}), \quad (1)$$

where τ is the loading time, N_0 is the maximal number of atoms in the trap. The cross-section is related to τ if there is only Rb in the vacuum chamber (which we assume):

$$\frac{1}{\tau} = n_{\text{Rb}} \sigma_{\text{Rb}} v_{\text{Rb}}, \quad (2)$$

where n_{Rb} is the number density, v_{Rb} is the average velocity of the Rb vapor (in the following, the subscript Rb is ignored).

As the luminescence-time signal also follows Eqn. 1, by fitting such a function to the oscilloscope data we have gathered yields τ :

$$\tau = (0.268 \pm 0.006) \text{ s}$$

With the recorded temperature $T = (293.55 \pm 0.05) \text{ K}$ and pressure $p = (8.09 \pm 0.01) \cdot 10^{-8} \text{ mbar}$,

$$v = \sqrt{\frac{2kT}{m}} = (293.545 \pm 0.025) \frac{\text{m}}{\text{s}}$$

The number density n can be calculated from the ideal gas law:

$$n = \frac{N}{V} = \frac{p}{kT} = (1.99704 \pm 0.00250) \cdot 10^{15} \frac{1}{\text{m}^3}$$

Finally, the cross-section:

$$\sigma = \frac{1}{n\tau v} = (6.355 \pm 0.131) \cdot 10^{-18} \text{ m}^2 \quad (3)$$

4.6 Influence of Laser Detuning

5 Conclusion

References

- ¹ C. Wieman, G. Flowers and S. Gilbert, *Am. J. Phys.* **63** (1995).
- ² Unspecified Author, *FP Experiment: Rubidium MOT* (University of Bonn, 2014).
- ³ H. Metcalf and P. van der Straten, *Laser Cooling and Trapping* (Springer, 1999).
- ⁴ C. Wieman and G. Flowers, *American Journal of Physics* **63** (1995), pp.317-30.
- ⁵ A. Wolski, *Maxwell's equations for magnets* (University of Liverpool, 2014), <https://arxiv.org/pdf/1103.0713.pdf>.
- ⁶ C. J. Foot, *Atomic Physics* (Oxford University Press, New York, 2005).
- ⁷ W. Demtröder, *Laser Spectroscopy, Basic Concepts and Instrumentation* (Springer, 2003).
- ⁸ *Physics Fundamentals: Laser Diode Characteristics*, <https://www.sukhamburg.com/download/fundamentals-laserdiodes.pdf>